XXVIII International Conference on Photonic, Electronic and Atomic Collisions (ICPEAC 2013) IOP Publishing
Journal of Physics: Conference Series **488** (2014) 012024 doi:10.1088/1742-6596/488/1/012024

Effects of autoionizing states on two-photon double ionization of the H_2 molecule

Xiaoxu Guan[1], Klaus Bartschat[1], Barry I. Schneider[2], and Lars Koesterke[3]

[1]Department of Physics and Astronomy, Drake University, Des Moines 50322, USA
[2]Division of Advanced Cyberinfrastructure, National Science Foundation, Arlington, Virginia 22230, USA
[3]Texas Advanced Computer Center, University of Texas at Austin, Austin, Texas 78758, USA

E-mail: xiaoxu.guan@drake.edu, klaus.bartschat@drake.edu, bschneid@nsf.gov, lars@tacc.utexas.edu

Abstract. Treating the effects of autoionizing intermediate states on two-photon double ionization (DI) of the H_2 molecule using time-dependent laser pulses is a significant computational challenge. Relatively long exposure times are critical to understanding the dynamics. Using the fixed-nuclei approximation, we demonstrate how the doubly excited states enhance the angle-integrated generalized cross sections in H_2, and how they affect the angular distribution pattern of the ejected electrons. As the energy approaches the threshold for sequential DI, there is a sharp rise in the cross section due to virtual sequential ionization.

1. Introduction

Few-photon multiple ionization of atoms and molecules irradiated by intense laser pulses has attracted growing interest in recent years. Such processes provide valuable information on the correlated response of multi-electron targets to strong driving laser fields in both the time and momentum domains. Two-photon double ionization (DI) in the noble gas neon and argon atoms was studied experimentally by Moshammer *et al.* [1].

Due to the lack of spherical symmetry and the entangled motions of the nuclei and the electrons, the situation in molecules is much more complicated than in atoms. As the simplest two-electron molecule, H_2 serves as a benchmark system to understand the intrinsic multi-center, multi-electron characteristics in laser-matter interaction. Only recently, the experimentally obtained spectrum of the nuclear fragments from H_2 after sequential DI at a photon energy of 38 eV was reported [2]. Observing the ejected electrons as well remains a major challenge.

On the theoretical front, the situation is also far from satisfactory. For a photon energy of 30 eV, specifically, there exist noticeable discrepancies among published results [3, 4, 5] for the generalized angle-integrated and angle-resolved cross sections for two-photon DI of H_2. Two more recent attempts at the problem [6, 7] add even more flavor and weight to the controversy.

Even if the degree of freedom in the nuclear motion is neglected, as is the case in the fixed-nuclei approximation (FNA) used in the present work, numerically treating two electrons in a two-center Coulomb potential is a significant challenge and requires considerable supercomputer resources. Also, caution needs to be exercised when extracting meaningful cross sections from


Content from this work may be used under the terms of the Creative Commons Attribution 3.0 licence. Any further distribution of this work must maintain attribution to the author(s) and the title of the work, journal citation and DOI.
Published under licence by IOP Publishing Ltd

both the time-dependent and time-independent approaches [8]. All published results from time-dependent approaches to date [3, 4, 6, 7, 9] were obtained with relatively short laser pulses with durations of $10-15$ optical cycles (o.c.) and peak intensities ranging from about 10^{13} to 10^{15} W/cm^2. For the total cross sections, the discrepancies between the time-dependent close-coupling (TDCC) results of Colgan *et al.* [4] and our recent predictions [3] obtained with a time-dependent finite-element discrete variable representation (TD FE-DVR) are about 25% and 80%, respectively, for the molecular axis aligned parallel and perpendicular to the linear polarization axis of the laser.

It is important to note, however, that results from time-dependent approaches may not be directly comparable either to each other or to those from time-independent calculations, due to a possible influence of the spectral character of the laser pulse. Time-independent models assume monochromatic radiation with infinite energy resolution while different pulse shapes (length and envelope) may have an effect as well. Provided the numerical aspects are under control, virtually the same results should, of course, be obtained when the same or very similar parameters are used in the time-dependent treatments. This was indeed confirmed by two recent time-dependent calculations [6, 7]. At the photon energy of 30 eV, the total cross sections of Simonsen *et al.* [6] and the triple-differential cross sections (TDCSs) of Ivanov and Kheifets [7] are in excellent agreement with ours [3] for both parallel and perpendicular configurations, when they were extracted with similar laser parameters.

A still open physical question in this field concerns possible effects of the doubly excited states (DESs) on two-photon DI of the H_2 molecule. In contrast to its atomic counterpart, helium, the doubly excited $Q_1\ ^1\Sigma_u^+$ series in H_2 can be accessed with extreme ultraviolet (xuv) radiation, while *only* the direct or non-sequential two-photon DI is open at the same time. If these DESs affect the cross sections, the question is to what extent and in what way, for example regarding the angular distribution. The present contribution addresses these fundamental issues in two-photon DI of the H_2 molecule, a highly correlated four-body Coulomb problem. We choose the case in which the laser polarization and the internuclear axis are parallel to illustrate these effects.

2. Theoretical Approach

Most theoretical methods are based on single-center expansions [4, 5, 6, 7] of the two-center problem in the fixed-nuclei approximation (FNA). While this expansion of the wave function is acceptable for the H_2 molecule, the numerical convergence of the results has to be carefully examined.

On the other hand, we formulate the problem in prolate spheroidal coordinates with the foci located on the two fixed nuclei. This is a natural and flexible system to capture the two-center characteristics. Generally, the total magnetic quantum number $M = m_1 + m_2$ along the molecular axis ($\boldsymbol{\zeta}$) is not a conserved quantity for the laser-driven H_2 molecule. Here m_1 and m_2 are the individual magnetic quantum numbers of the two electrons along the $\boldsymbol{\zeta}$ direction. The field-free Hamiltonian for each electron (ξ_q, η_q, $q = 1, 2$) is given by

$$\mathcal{H}_q = -\frac{2}{R^2(\xi_q^2-\eta_q^2)}\left[\frac{\partial}{\partial\xi_q}(\xi_q^2-1)\frac{\partial}{\partial\xi_q}+\frac{\partial}{\partial\eta_q}(1-\eta_q^2)\frac{\partial}{\partial\eta_q}+\frac{1}{(\xi_q^2-1)}\frac{\partial^2}{\partial\varphi_q^2}+\frac{1}{(1-\eta_q^2)}\frac{\partial^2}{\partial\varphi_q^2}\right]-\frac{4\xi_q}{R(\xi_q^2-\eta_q^2)}, \tag{1}$$

where R stands for the internuclear separation distance. The time-dependent Schrödinger equation (TDSE) in the electric field $\boldsymbol{E}(t)$ is given by

$$i\frac{\partial}{\partial t}\Psi(1,2,t) = \left[\mathcal{H}_1+\mathcal{H}_2+\frac{1}{r_{12}}+\boldsymbol{E}(t)\cdot(\boldsymbol{r}_1+\boldsymbol{r}_2)\right]\Psi(1,2,t). \tag{2}$$

We first expand the wave function in terms of $\Phi_{m_1m_2} = e^{im_1\varphi_1}e^{im_2\varphi_2}/(2\pi)$, with φ_1 and φ_2 being the azimuthal angles, i.e.,

$$\Psi(1,2,t) = \sum_{m_1m_2} \Pi_{m_1m_2}(\xi_1,\eta_1,\xi_2,\eta_2,t)\Phi_{m_1m_2}(\varphi_1,\varphi_2). \tag{3}$$

The two-electron wave function is then further expanded in terms of the FE-DVR bases $\{f_i(\xi)\}$ and $\{g_k(\eta)\}$ for both the "radial" (ξ_1, ξ_2) "angular" (η_1, η_2) coordinates at the fixed internuclear separation (1.4 bohr in our case). We have

$$\Pi_{m_1m_2}(\xi_1,\eta_1,\xi_2,\eta_2,t) = \sum_{ijk\ell} f_i(\xi_1)f_j(\xi_2)g_k(\eta_1)g_\ell(\eta_2)C^{m_1m_2}_{ijk\ell}(t). \tag{4}$$

Since we use the same set of DVR mesh points for all the m_i ($i = 1, 2$), the boundary conditions for even and odd m_i need to be properly incorporated in the DVR bases. An appealing feature of this representation lies in the fact that the expansion coefficients $C^{m_1m_2}_{ijk\ell}(t)$ in the (m_1m_2) channels have a very concise and transparent meaning. They are simply proportional to the values of the wave function at the predetermined grid points $(\xi_{1i}, \eta_{1k}, \xi_{2j}, \eta_{2\ell})$.

The TDSE is solved by propagating the wave function of the laser-driven system in time. Specifically, we employ the well-developed short-iterative Lanczos algorithm constructed in a Krylov subspace to generate the time-dependent wave function. We refer the reader to Refs. [3, 10] for more detailed presentations and discussions regarding the implementation of the FE-DVR formalism in two-electron molecules, in particular, the treatment of $1/r_{12}$ in two-center prolate spheroidal coordinates.

In the FNA, the DESs in molecules are not necessarily autoionizing due to the fact that the potential energy curves may cross with those of the parent ion (H_2^+ in our case). At the equilibrium internuclear distance of 1.4 bohr, however, the doubly excited $Q_1\ ^1\Sigma_u^+$ series lie below the $2p\sigma_u$ curve of the H_2^+ ion and hence the states decay into the single-ionization (SI) channel via autoionization. Due to the limited energy bandwidth and the lifetime of the DESs, properly resolving a possible effect of the intermediate DESs on the cross sections requires sufficiently long laser pulses. This, in turn, leads to a very large configuration space and hence requires significant computational resources. For a laser pulse lasting 40 optical cycles (o.c.), for example, spatial boxes reaching to $\xi_{\max} \approx 400$ are needed to obtain accurate results. The cross sections shown below were also extracted from an even larger box of $\xi_{\max} = 650$ (corresponding to $r_{\max} \approx 450$ bohr), in order to ensure that the results have converged properly.

3. Example Results and Discussions

3.1. Coplanar geometry

The coplanar geometry plays a critical role in understanding the dominant mode in double photoionization. Figure 1 illustrates this geometry, in which all relevant vectors are located in the same plane, also containing the molecular axis. In the two panels, the fixed electron with momentum $\boldsymbol{k}_1$ is detected in a direction either along or perpendicular to the linear polarization vector. The geometry is shown in the laboratory frame. However, the scattering information can be converted to the body frame, in which the momenta of photoelectrons and the $\boldsymbol{\epsilon}$ direction are measured with respect to the molecular axis.

3.2. Generalized cross sections

All published time-dependent results for the total cross sections to date are limited to very short laser pulses, lasting about $10 - 15$ o.c. In the present work, we carried out a systematic study to investigate how the predicted cross sections depend on the duration of the pulse. Figure 2

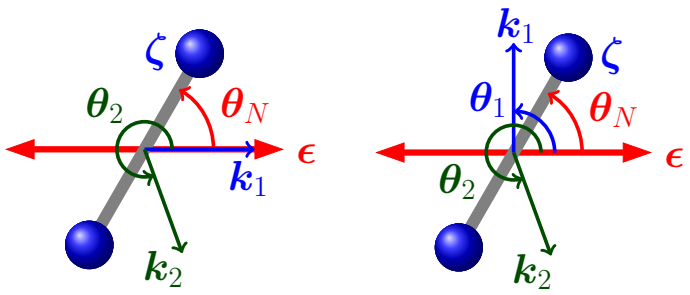

Figure 1. Coplanar geometry for DI. The molecular axis ($\boldsymbol{\zeta}$), the direction of laser polarization vector ($\boldsymbol{\epsilon}$), and the momenta $\boldsymbol{k}_1$ and $\boldsymbol{k}_2$ are located in the same plane. The angle θ_N stands for the alignment angle of the molecular axis with respect to the polarization direction.

displays the total cross section for photon energies ranging from 26.5 eV to 34.9 eV. As seen from the figure, no particular structure appears in the energy dependence of the total cross section in the DI domain for a relatively short pulse of, e.g., 10 cycles. Increasing the pulse duration, however, has a significant affect on the predicted cross sections.

Several aspects of these results deserve more discussion. To begin with, the cross sections for photon energies around 30.5 eV are significantly enhanced if the pulse duration is longer than 20 o.c., and a broad shoulder develops around 32.5 eV. The bandwidth of the 30.15-eV pulse is 1.5 eV in the 40-cycle case. This is approximately three times wider than the energy width ($\simeq 0.443$ eV [11]) of the first doubly excited $Q_1\ ^1\Sigma_u^+$ state at $R_{\rm eq}$ of 1.4 bohr. The pulse length of 5.49 fs for 40 cycles of the laser interaction is thus three times longer than the lifetime (1.48 fs) of the first DES. This allows for autoionizing states to decay into the channel $H_2^+(^2\Sigma_g^+) + e^-(El\lambda)$ even before the end of the laser pulse. The features seen are thus essentially due to intermediate resonances associated with the first, second, and higher-lying doubly excited states in the $Q_1\ ^1\Sigma_u^+$ series. The first DES in the above series manifests itself as a resonance peak observed around 30.5 eV. The second peak in the cross section at the photon energy of 32.5 eV corresponds to the second and higher-lying DESs. The 40-cycle xuv pulse has a sufficiently narrow energy bandwidth to properly resolve the first resonance. For the shoulder around 32.5 eV, on the other hand, we can only observe a cluster generated by the second and higher-lying DESs.

The longer pulse duration allows for autoionizing decays of the DESs into the SI channel to be observable in the time domain. The hydrogen molecule is a unique system that exhibits interference in the two-photon direct DI with the DESs. This is in contrast to the helium atom,

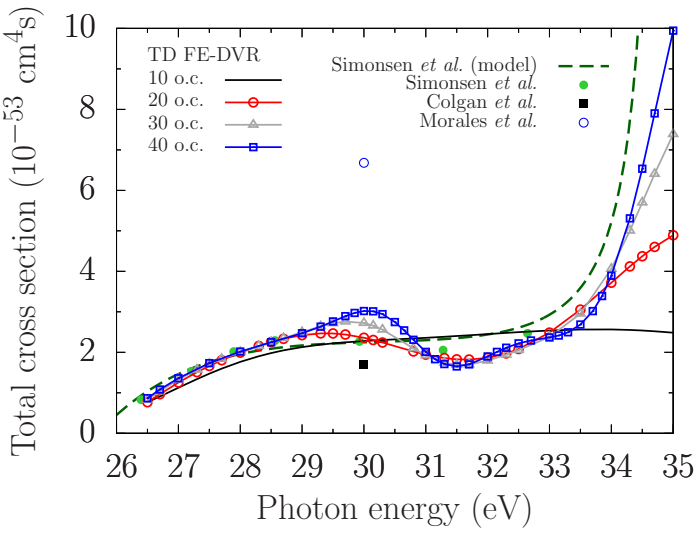

Figure 2. Angle-integrated generalized cross section for two-photon DI of H_2 at the equilibrium internuclear separation of 1.4 bohr. The molecular axis is oriented along the direction of the polarization vector. The present results obtained with the TD FE-DVR method are shown as lines with symbols for pulse durations ranging from 10 o.c. (1.2 − 1.6 fs) to 40 o.c. (4.7 − 6.2 fs). The results of Simonsen *et al.* (*ab-initio* and model) [6], Colgan *et al.* [4], and Morales *et al.* [5] are presented as well.

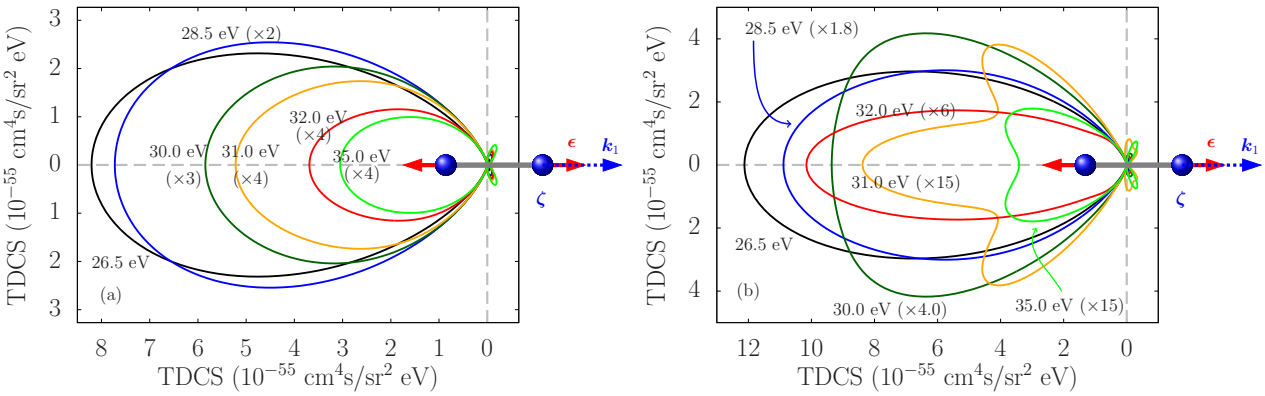

Figure 3. Angular distributions of electrons ejected from the H_2 molecule at equal energy sharing. Panels (a) and (b) correspond to 10 o.c. and 40 o.c., respectively. The fixed electron (momentum $\boldsymbol{k}_1$) is observed along the direction of the polarization vector, which is chosen parallel to the molecular axis. Each angular distribution has been scaled individually as indicated.

where the DESs are populated either using two-color laser pulses or higher photon energies in the sequential domain of two-photon DI.

Another interesting aspect concerns the near-threshold behavior when the photon energy approaches the threshold of sequential DI at 34.9 eV (in the FNA at the equilibrium distance). Increasing the interaction time results in a sharp rise of the total cross section near the sequential threshold. This energy dependence is essentially the same as that observed in the helium atom. The mechanism behind this phenomenon, termed "virtual" two-photon sequential DI [12], is attributed to highly asymmetric energy distributions near the opening of the sequential DI channel. A simple model used by Simonsen *et al.* [6], based on a suggestion by Horner *et al.* [13], essentially captures this behavior.

We now turn to the effect of the DESs on the emission modes for two-electron ejection. The TDCSs for equal-energy sharing are depicted in Fig. 3. As expected, the TDCSs are essentially

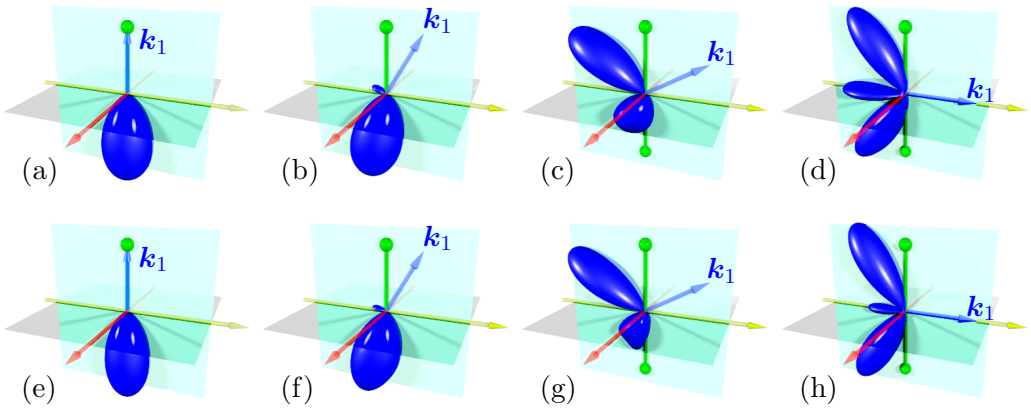

Figure 4. Angular distributions of the electrons ejected from the H_2 molecule at equal energy sharing. The photon energy is 26.5 eV. Panels (a)-(d) and (e)-(h) correspond, respectively, to 10 o.c. and 40 o.c. The fixed electron (momentum $\boldsymbol{k}_1$) is observed at angles of 0°, 30°, 60°, 90° with respect to the molecular axis. Each angular distribution has been scaled individually.

back-to-back. This mode of emission is valid for photon energies near the opening of the channel for direct DI all the way to the threshold for sequential DI. Compared to the shorter interaction time of 10 o.c., however, additional features appear for the longer time duration of 40 cycles if the photon energy falls into the resonance regime, for instance at 31.0 eV. While the dominant back-to-back mode remains, interference with the decay of the intermediate DES changes the patterns in the TDCSs significantly. The details are clearly sensitive to both the pulse duration and the photon energy.

Figure 4 shows the angular distributions at the photon energy of 26.5 eV, which is near the threshold for the direct two-photon DI to open. In this case, neither the shape nor the magnitude of the angular distribution is very sensitive dependent on the pulse duration. Angular distributions in the resonance regime will be presented elsewhere [14].

4. Conclusion and Outlook

We have explored critical time-scale issues regarding the laser pulse in two-photon direct DI of the H_2 molecule. DES effects on the predicted angle-integrated and angle-resolved cross sections were identified by using longer than usual interaction times. While currently limited to the fixed-nuclei approximation, the progress reported in the present work is an important step towards fully understanding the correlated response of the nuclear fragments and the ejected electrons to intense laser fields. In order to directly compare with experimental data, which may become available in the foreseeable future, the nuclear motion will need to be accounted for. Work in this direction is currently in progress in our group.

Acknowledgments

We gratefully acknowledge Dr. M. Førre for sending results in electronic form and helpful discussions. We also thank Drs. R. Moshammer, R. Dörner, and M. Meyer for clarifying aspects regarding the prospects for an experimental investigation of this problem. This work was supported by the NSF under grant No. PHY-1068140 (XG and KB) and supercomputer resources through the XSEDE Allocation PHY-090031.

References

[1] R. Moshammer *et al.*, Phys. Rev. Lett. **98**, 203001 (2007).
[2] Y. H. Jiang *et al.*, Phys. Rev. A **81**, 021401(R) (2010).
[3] X. Guan, K. Bartschat, and B. I. Schneider, Phys. Rev. A **82**, 041404(R) (2010).
[4] J. Colgan, M. S. Pindzola, and F. Robicheaux, J. Phys. B **41**, 121002 (2008).
[5] F. Morales, F. Martín, D. A. Horner, T. N. Rescigno, and C. W. McCurdy, J. Phys. B **42**, 134013 (2009).
[6] A. S. Simonsen, S. A. Sørngård, R. Nepstad, and M. Førre, Phys. Rev. A **85**, 063404 (2012).
[7] I. A. Ivanov and A. S. Kheifets, Phys. Rev. A **87**, 023414 (2013).
[8] X. Guan, K. Bartschat, and B. I. Schneider, Phys. Rev. A **77**, 043421 (2008).
[9] X. Guan, K. Bartschat, and B. I. Schneider, Phys. Rev. A **84**, 033403 (2011).
[10] X. Guan, K. Bartschat, and B. I. Schneider, Phys. Rev. A **83**, 043403 (2011).
[11] I. Sánchez and F. Martín, J. Chem. Phys. **106**, 7720 (1997).
[12] P. Lambropoulos, L. A. A. Nikolopoulos, M. G. Makris, and A. Mihelič, Phys. Rev. A **78**, 055402 (2008).
[13] D. A. Horner, F. Morales, T. N. Rescigno, F. Martín, and C. W. McCurdy, Phys. Rev. A **76**, 030701(R) (2007).
[14] X. Guan, K. Bartschat, B. I. Schneider, and L. Koesterke, Phys. Rev. A **88**, 043402 (2013).